

MIT Open Access Articles

Trajectory-based Deformation Correction in Ultrasound Images

The MIT Faculty has made this article openly available. **Please share** how this access benefits you. Your story matters.

Citation: Sun, Shih-Yu, Brian W. Anthony, and Matthew W. Gilbertson. "Trajectory-based deformation correction in ultrasound images." *Medical Imaging 2010: Ultrasonic Imaging, Tomography, and Therapy*. Ed. Jan D'hooge & Stephen A. McAleavey. San Diego, California, USA: SPIE, 2010. 76290A-9. © 2010 SPIE.

As Published: <http://dx.doi.org/10.1117/12.844184>

Publisher: SPIE

Persistent URL: <http://hdl.handle.net/1721.1/58562>

Version: Final published version: final published article, as it appeared in a journal, conference proceedings, or other formally published context

Terms of Use: Article is made available in accordance with the publisher's policy and may be subject to US copyright law. Please refer to the publisher's site for terms of use.



Trajectory-based Deformation Correction in Ultrasound Images

Shih-Yu Sun, Brian W. Anthony*, Matthew W. Gilbertson
Laboratory for Manufacturing and Productivity, MIT, Cambridge, MA, 02139

ABSTRACT

Tissue deformation in ultrasound imaging poses a challenge to the development of many image registration techniques, including multimodal image fusion, multi-angle compound image and freehand three-dimensional ultrasound. Although deformation correction methods are desired to provide images of uncompressed tissue structure, they have not been well-studied. A novel trajectory-based method to correct a wide range of tissue deformation in ultrasound imaging was developed. In order to characterize tissue deformation under different contact forces, a force sensor provides contact force measurement. Template based image-flow techniques were applied to RF A-lines under different contact forces. A two-dimensional displacement trajectory field was constructed, where pixel coordinates in each scan were plotted against the corresponding contact force. Nonlinear extrapolation algorithms are applied to each trajectory to relocate the corresponding pixel to where it would have been had there been no contact, thereby correcting tissue deformation in the images. This method was validated by using a combination of FEM deformation and ultrasound simulation. It was shown that deformation of the simulated pathological tissue could be corrected. Furthermore, nonlinear polynomial regression was found to give better estimates, than linear regression, when large deformation was present. Estimation accuracy was not improved significantly for a polynomial regression larger than second order.

Keywords: deformation correction, 2D displacement estimation, trajectory, soft tissue modeling, hyperelastic, non-rigid registration

1. INTRODUCTION

Ultrasound imaging is regularly used for diagnosis, and is usually performed in a manner where a probe makes contact with the skin. In this procedure, deformation of the underlying tissue is inevitable, and thus structures shown in imaging are actually distorted. The distortion is usually small and would not be a problem in most situations, since most of the characteristics of tissue will be retained under compression. In fact, tracking tissue deformation under probe contact provides information to discriminate between normal and pathological tissue in elastography.

For applications where the undeformed appearance of biological tissue is required, however, correcting or avoiding tissue deformation becomes important. For example, in freehand three-dimensional ultrasound (freehand 3D US), where the shape of tissue is reconstructed by stacking two-dimensional (2D) slices acquired in varying probe positions and contact forces, the corresponding pixels can be accurately aligned only if different deformation patterns in each slice can be appropriately corrected. Furthermore, deformation correction applied in 3D US facilitates accurate quantitative measurement of volumes and tissue shape analysis. The need to correct deformation also arises in multimodal image processing, in which tissue deformation in ultrasound scanning has to be corrected before the image can be accurately registered with those from other modalities.

Several deformation correction methods have been reported, aiming to estimate zero-force images that would have been acquired as if there had been no probe contact. In the method proposed by Treece et al.¹, probe position measurement was combined with image-based registration to correct deformation along the axial direction. Burcher et al. proposed the *a priori* finite-element method (FEM) model that could predict and correct tissue deformation in both the axial and lateral directions, which incorporated *a priori* knowledge of tissue elasticity and contact force measurement.² A two-dimensional deformation correction method, for reducing dependence on elastic property assumptions, based on speckle tracking and pixel trajectories was described by Burcher³. In this method, linear dynamics was used for describing the mechanical behaviors of biological tissue under compression, which is only applicable over a small range of contact forces.

*banthony@csail.mit.edu

In this paper, a novel trajectory-based deformation correction method, incorporating contact force measurement and two-dimensional displacement estimation, is described. This method aims to provide an accurate model of biological tissue deformation, and to be applicable to correcting large tissue deformation. The method was validated by a numerical phantom study; the performance of deformation correction is analyzed by contour extraction and area estimation.

2. METHODS

In order to characterize tissue deformation, pixel displacement estimation was performed between ultrasound images under different contact forces. Knowledge of contact force and the corresponding pixel displacements allowed the construction of a trajectory field for the specific subject under an ultrasound scan. Pixel coordinates in the scan planes were plotted against the corresponding contact forces. After the trajectory field was built, an extrapolation algorithm was applied on each pixel-trajectory to relocate the pixel to where it would have been had there been no contact force, thereby reconstructing the undeformed tissue appearance. This method was validated by using FEM and ultrasound simulation. The essential steps of this procedure are described in the following subsections.

2.1 Displacement field estimation

Tissue deformation due to probe compression was estimated by pixel displacement fields, which described how each part of tissue moved when a certain contact force was applied. For characterizing force-varying deformation patterns, a set of displacement fields were established by tracking each pixel over the whole field of view along a sequence of ultrasound images under varying contact forces, as shown in Figure 1.

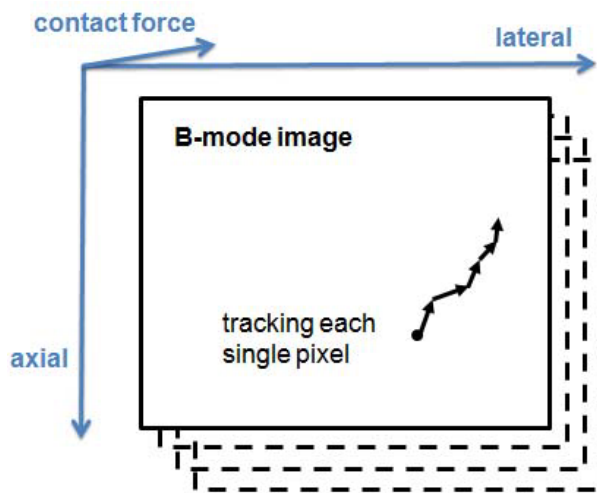


Figure 1. Tissue deformation states could be modeled by tracking each single pixel in the field of view along the B-mode image sequence under varying contact forces.

A 2D displacement estimation algorithm was implemented based on the template-matching method proposed by Zahiri-Azar et al.⁴ In this method, pre-compression RF A-lines were axially divided into overlapping windows with a length of 1mm. Each windowed pre-compression segment was then compared with the corresponding post-compression RF A-line in order to find the most similar segment; normalized cross correlation was used as a similarity measure. Interpolation was performed on the sampled cross correlation functions in order to achieve sub-sample accuracy displacement estimation. Cosine curve fitting through three sample points was used as the interpolation scheme.⁵ Finally, instead of applying the 1D procedure in the axial and lateral directions independently, estimation in the lateral direction was performed only after the axial displacement was determined, since pixel displacements in the two directions are physically coupled.

2.2 Trajectory field and extrapolation

A trajectory field is then established by plotting the 2D coordinates of each pixel against the corresponding contact force, as shown in Figure 2. The location where a pixel would have been if there had been no contact force is estimated by finding the intersection of the corresponding trajectory and the “zero-force” plane. Through application of this algorithm to all pixels in the trajectory field, deformation of tissue in the image is corrected.

Both linear and nonlinear polynomial extrapolation methods were tested in this study because it has been widely reported that, when compressed, biological tissue exhibits significant nonlinear mechanical behaviors⁶, whose characterization might require more than one degree of freedom. The results of this regression analysis are described in section 3. **RESULTS AND DISCUSSION**.

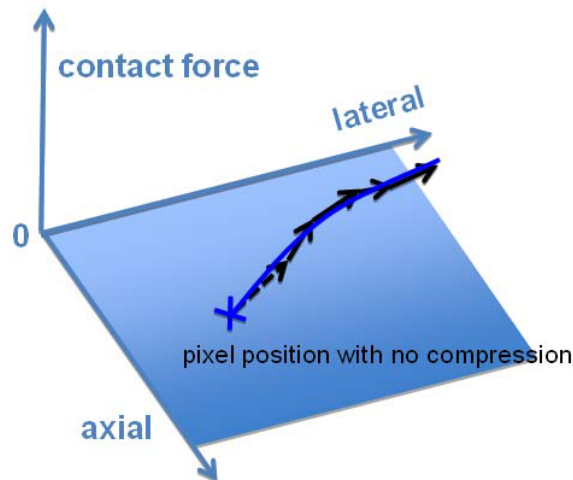


Figure 2. The B-mode image that one would have acquired if there had been no contact could be reconstructed by performing extrapolation over the trajectory field, which describes pixel movement with changing contact force.

2.3 Numerical phantom study

Performance of the deformation correction method was validated through the use of FEM and the ultrasound simulation software Field II.⁷⁻⁸ A numerical phantom was built in FEM in order to simulate the mechanical behaviors of breast tissue under probe contact. A corresponding phantom was built in Field II for simulating B-mode images of the numerical phantom in FEM under varying deformation states. Finally, those B-mode images, as well as the contact force measurements in FEM, were used to build a trajectory field for estimating the undeformed appearance of the simulated pathological tissue embedded in the phantom.

2.3.1 Finite-element method (FEM)

A 100mm × 60mm numerical phantom that simulated breast tissue was built in commercial FEM software (Abaqus 6.8, HKS, Rhode Island). Inside the phantom, a circular region with a radius of 7.5mm was set to have higher stiffness for mimicking pathological tissue, and its center was placed 22.5mm below the top surface of the phantom, as shown in Figure 3. Consistent with the displacement estimation method described earlier, which ignored displacement in the elevational direction (perpendicular to the scan plane), the FEM modeling and simulation were set to be two-dimensional, that is, in the axial and lateral directions.

Here the mechanical behaviors of the phantom undergoing finite strains were described by hyperelastic models. In addition, the phantom was assumed to be isotropic and incompressible. Out of several models that characterize such

material, the Neo-Hookean model was chosen for simulation. The model can be described by the strain energy potential function in Equation (1).

$$U = C_{10}(\bar{I}_1 - 3) \quad (1)$$

where U is the strain energy per unit volume, \bar{I}_1 is the first deviatoric strain invariant, and C_{10} is the material parameter. According to previously reported *ex-vivo* experimental results⁶, the value $3.1 \times 10^{-4} \text{ N/mm}^2$ was assigned to the parameter C_{10} for the region in the phantom that mimicked normal breast tissue, and four times that value were used for the harder inclusion for mimicking pathological tissue.

A rigid indenter mimicking an ultrasound probe (vermon LA 5.0/128-522) was modeled and used to compress the phantom against the rigid plane at the bottom. It should be noted that, in ultrasound scanning, the subject is scanned with respect to the probe. Therefore, features in the phantom would seem to be moving upward in the image when being compressed, while they would actually move downward physically. In order to simulate tissue deformation measured in the coordinate system of the probe, in the compression simulation the probe was fixed, while the rigid plane was set to be moving upward.

The numerical phantom was a mesh of 3724 plane strain quadrilateral elements with 3825 nodes. Compression and the resulting tissue deformation were then simulated in a quasi-static manner for describing very slow motion and ignoring inertial effects.

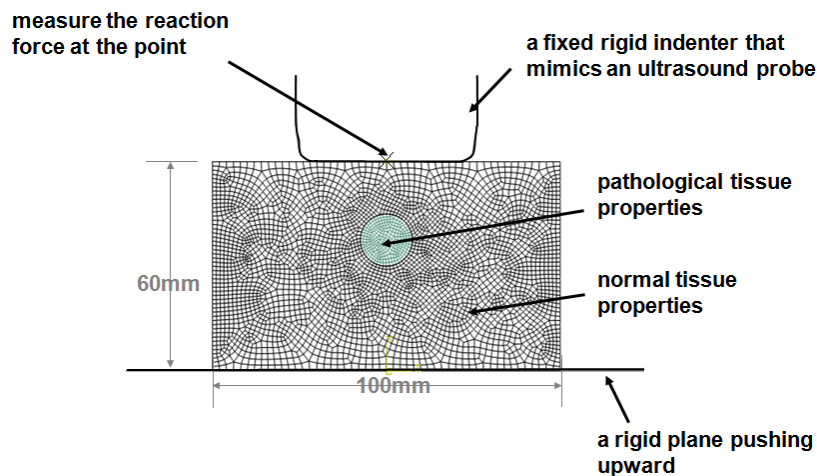


Figure 3. The setup in FEM is shown. A harder inclusion was embedded in the numerical phantom for mimicking pathological tissue. For simulating probe compression, the probe was fixed and the bottom rigid plane pushed upward, since the scan plane follows the coordinate system of the probe.

2.3.2 Ultrasound simulation

For simulating the B-mode images of the numerical phantom in FEM, a corresponding phantom was modeled in the ultrasound simulation software Field II. 2×10^5 scatterers were randomly distributed in a $100\text{mm} \times 60\text{mm} \times 10\text{mm}$ cube. The top surface of the phantom was 30mm below the probe. A sampled set of the scatterers is shown in Figure 4. The circular region marked in blue corresponded to the simulated pathological tissue in FEM, and the region was set to have a higher average of acoustic impedance in Field II. The rectangular region bounded by dashed lines indicates the field of view in the simulated ultrasound scanning.

In order to simulate B-mode images of the numerical phantom in varying deformation states, the results of nodal displacement measurement in FEM deformation analysis were linearly interpolated to relocate the scatterers to where they would be if the phantom were compressed. Here in the simulation, a linear probe array was modeled, with a center

frequency of 5MHz and a sampling rate of 60MHz, and the transmit focus was set to be 55mm in depth. The pitch of the probe array was 0.3mm, and 64 elements were used for every scan line. An image was composed of 128 scan lines, with a spatial spacing of 0.3mm in the lateral direction.

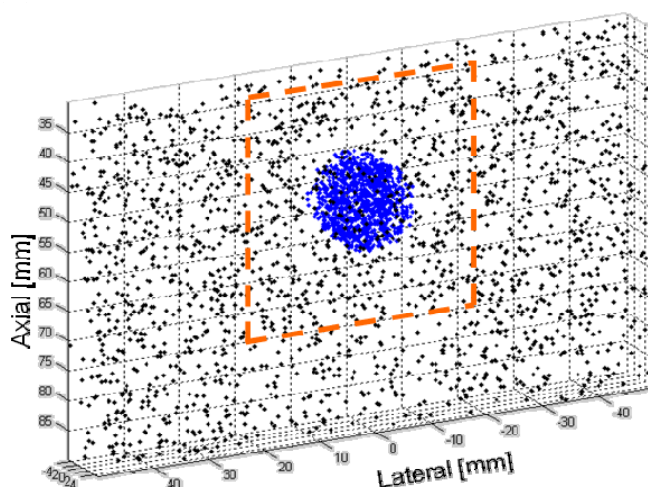


Figure 4. A sampled set of the scatterers of the phantom in ultrasound simulation is shown. The region bounded by dashed lines indicates the field of view, and the region marked in blue corresponds to the simulated pathological tissue in FEM.

3. RESULTS AND DISCUSSION

For validating the proposed deformation correction method, ten B-mode images were simulated from compression of the numerical phantom in FEM by 5mm to 14mm, with a spacing of 1mm. The reaction forces sensed by the probe in the compression simulations were also calculated. The trajectory field between the ten images was then determined after the displacement fields between consecutive B-mode images were estimated and median-filtered with a 15x15 kernel. Although an arbitrary selection out of the ten images (5mm to 14mm compression) could be used for estimating the uncompressed inclusion appearance, the results of correcting the image under 14mm compression, which corresponds to a large strain of over 20%, are shown here as an example.

The performance of correcting for 14mm compression was examined through comparison of the inclusion contours in the corrected and uncorrected images. The contours were extracted by the Gradient Vector Flow for Snake (GVF-snake) algorithm⁹. The GVF algorithm uses diffusion of the gradient vectors derived from gray-level edge maps as an external force for active contour fitting. The snakes were initialized by the use of an interactive graphical user interface (GUI), and then gradually shrunk to delineate the edges of the inclusions by iteration. The squared magnitudes of the gradient fields derived from the B-mode images were used as the edge maps. The GVF-snake algorithm has been shown to be relatively insensitive to contour initialization, and to be able to converge to boundary concavities. The GVF-snake software is available at <http://iacl.ece.jhu.edu/projects/gvf>.

Figure 5 shows the results of correction by the use of linear regression for extrapolation on the trajectory field. It can be seen that both the shape and position of the compressed inclusion deviated significantly from those of the inclusion in the uncompressed state. These deviations were largely removed after linear correction. The improvement in estimating the uncompressed inclusion contour was further quantified by three parameters that characterize area estimation error: true positive (TP), false negative (FN), and false positive (FP).¹⁰ Those parameters are illustrated in Figure 6. From Table 1, the area estimation error parameters improved significantly after linear deformation correction.

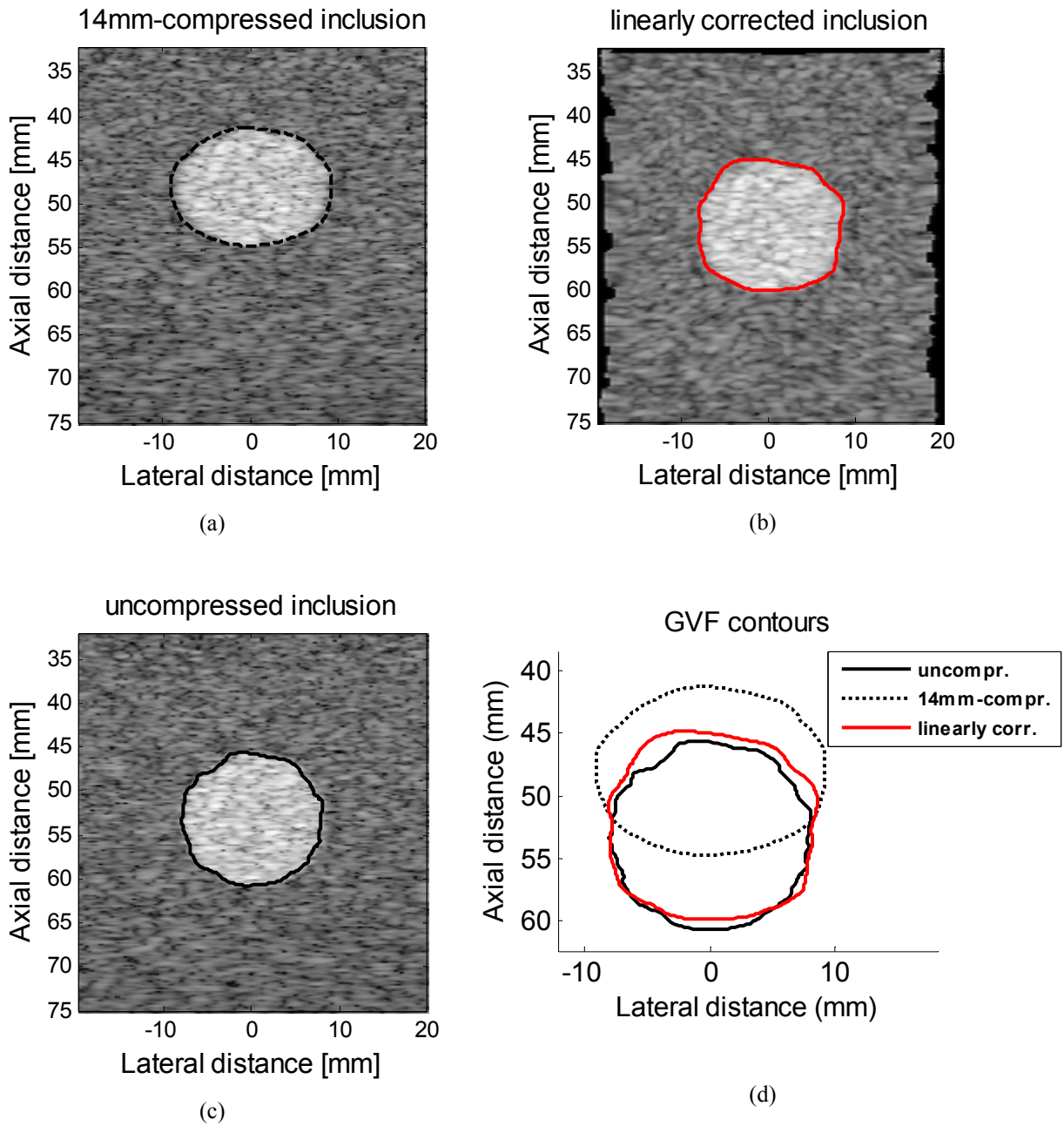


Figure 5. The B-mode image of the 14mm-compressed inclusion (a) was linearly corrected (b). From the comparison between (a), (b) and the true uncompressed inclusion contour (c), it was shown that the proposed method could largely restore the shape and position of the inclusion to its uncompressed state. (d)

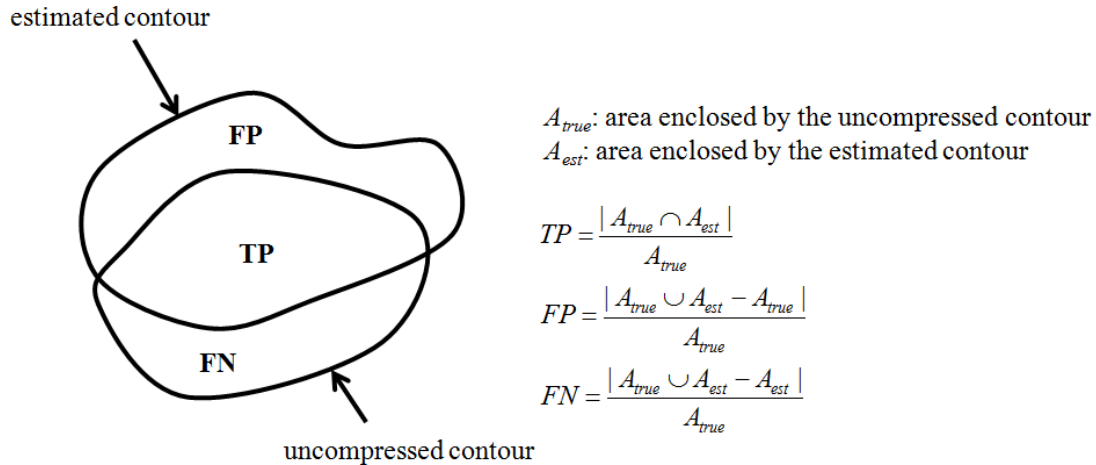


Figure 6. The performance of deformation correction was quantified by three parameters that were derived from area estimation. They are true positive (TP), false positive (FP), and false negative (FN).

Table 1. The area estimation parameters derived from comparing the 14mm-compressed and the linearly corrected contours with the true uncompressed contour in Figure 5.

	TP	FN	FP
14mm compression	0.56	0.44	0.49
linear correction	0.96	0.04	0.13

The performance of deformation correction by nonlinear polynomial regression was also examined. The image of 14mm-compressed numerical phantom was corrected by the use of polynomial regression of order one to four. Then a GVF snake was initialized to extract the inclusion contours in the four corrected images, as well as the image in the uncompressed state. The contour extraction procedure was repeated ten times, in each of which a different initial GVF snake was used. The initial snakes were drawn in a manner that all of the five inclusions would be enclosed.

Figure 7(a) shows a typical example with the extracted contours overlaid. The contours from 2nd- to 4th- order regressions varied insignificantly and were close to the uncompressed contour. There was noticeable deviation between the contours from linear and nonlinear regressions.

Figures 7(b)-(d) show the area estimation parameters derived from results of the ten contour extraction procedures, where the error bars indicate standard deviations in each measure. By paired t-test, it was shown that nonlinear polynomial regression outperformed linear regression ($p < 10^{-10}$ for all three parameters.) In addition, the 3rd-order polynomial regression gave better TP and FN measures than the others ($p < 10^{-5}$), while in terms of FP, the difference between 3rd-order regression and the other nonlinear ones was not statistically significant. Therefore, considering both performance of correction and the required computational cost, 2nd-order polynomial regression should make the best balance.

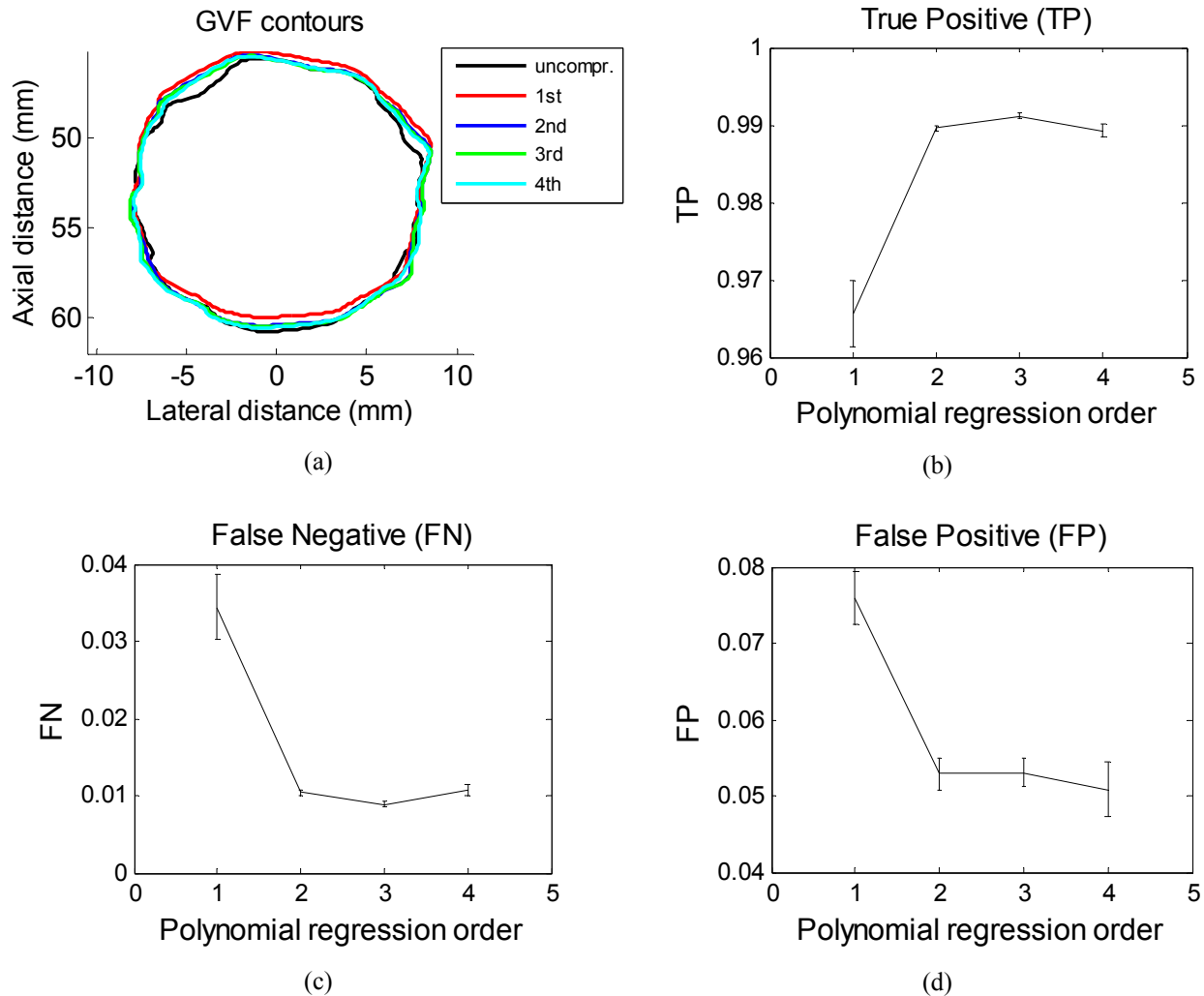


Figure 7. Comparison of the inclusion contours after deformation correction incorporating 1st-, 2nd-, 3rd-, or 4th-order polynomial regression is shown. (a) From the area estimation parameters (b)-(d), nonlinear regression gave better estimation accuracy than linear regression, but an order higher than two did not lead to improvement in performance.

4. CONCLUSION

In this study, a novel method for correcting tissue deformation in ultrasound images was presented. It involves measuring the contact force between the probe and skin surface while performing an ultrasound scan. A 2D trajectory field is estimated from displacement fields between consecutive scans and contact force measurements. Tissue deformation in the B-mode images is then corrected by extrapolating pixel trajectories back to zero force.

This method was evaluated by FEM and ultrasound simulation, in which a harder inclusion was embedded in the numerical phantom for mimicking pathological tissue. It was shown that the proposed method could reconstruct the appearance of the uncompressed inclusion in semi-automatic contour extraction. Furthermore, when correcting large deformation with a strain of over 20%, the method was found to perform better when nonlinear polynomial regression was used for extrapolation, although a polynomial order higher than two did not give better accuracy in area estimation.

ACKNOWLEDGEMENT

The research was sponsored by Singapore-MIT Alliance (SMA). The authors also thank Terason for donating the t3000 ultrasound imaging system and their technical support.

REFERENCES

- [1] Treece, G.M., Prager, R.W., Gee, A.H., and Berman, L., "Correction of probe pressure artifacts in freehand 3D ultrasound," *Medical Image Analysis* 6, 199–214 (2002).
- [2] Burcher, M.R., Han, L. and Noble, J.A., "Deformation correction in ultrasound images using contact force measurements," *Proceedings of the IEEE Workshop on Mathematical Methods in Biomedical Image Analysis (MMBIA'01)* 63 (2001).
- [3] Burcher, M., [A Force-based Method for Correcting Deformation in Ultrasound Images of the Breast], University of Oxford, (2002).
- [4] Zahiri-Azar, R. and Salcudean, S.E., "Real-time estimation of lateral displacement using time domain cross correlation with prior estimates," *IEEE Ultrasonics Symposium*, 2006 1209–1212 (2006).
- [5] Zahiri-Azar, R., Goksel, O., Yao, T.S., Dehghan, E., Yan, J., and Salcudean, S.E., "Methods for the estimation of sub-sample motion of digitized ultrasound echo signals in two dimensions," *EMBS 2008. 30th Annual International Conference of the IEEE* 5581–5584 (2008).
- [6] Samani, A. and Plewes, D., "A method to measure the hyperelastic parameters of ex vivo breast tissue samples," *Physics in Medicine and Biology* 49, 4395–4406 (2004).
- [7] Jensen, J.A. and Svendsen, N.B., "Calculation of pressure fields from arbitrarily shaped, apodized, and excited ultrasound transducers," *IEEE Transactions on Ultrasonics, Ferroelectrics and Frequency Control* 39, 262–267 (1992).
- [8] Jensen, J.A., "Field: A program for simulating ultrasound systems," *Medical and Biological Engineering and Computing* 34, 351–352 (1996).
- [9] Xu, C. and Prince, J.L., "Snakes, shapes, and gradient vector flow," *IEEE Transactions on image processing* 7, 359–369 (1998).
- [10] Madabhushi, A. and Metaxas, D.N., "Combining low-, high-level and empirical domain knowledge for automated segmentation of ultrasonic breast lesions," *IEEE transactions on medical imaging* 22, 155–169 (2003).